Proceedings of the 17th World Congress
The International Federation of Automatic Control
Seoul, Korea, July 6-11, 2008

Preliminary Experiments of GPS/INS Based Integrity Monitoring Using MSAS Differential Correction Data

T. Tsujii*. H. Tomita*. T. Fujiwara*. and M. Harigae*

*Aviation Program group, Japan Aerospace Exploration Agency,
Tokyo, Japan (Tel: +81-422-40-3605; e-mail: tsujii@ chofu.jaxa.jp).

Abstract: Japan Aerospace Exploration Agency (JAXA) has developed several GPS/INS systems called GAIA (GPS Aided Inertial navigation Avionics) for over ten years and succeeded in automatic landing of unmanned experimental vehicle in differential mode. In order to use GAIA for civil aviation, JAXA has been developing a fault detection and exclusion (FDE) software for integrity monitoring based on filter bank method. On the other hand, a Japanese satellite based augmentation system, MSAS (MTSAT Satellite-based Augmentation System) is planned to be operational in 2007, and the test signal is transmitted. A flight experiment to collect MSAS data was conducted and GPS/MSAS data were used to compute horizontal protection level (HPL). The GPS/INS filter bank method showed a reduced HPL, compare to MSAS-based HPL.

1. INTRODUCTION

GPS/INS integrated navigation system has been a candidate of integrity monitoring system since an inertial sensor could improve performance of the fault detection and exclusion (FDE) functions. JAXA has developed several GPS/INS systems called GAIA (GPS Aided Inertial navigation Avionics) for over ten years and succeeded in automatic landing of unmanned experimental vehicle in differential mode. Although high accuracy at the level of Category III approach and landing was achieved, GAIA could not be used for civil aviation since its integrity was not ensured. Therefore, JAXA has commenced research on FDE algorithms for GPS/INS navigation system, and a prototype software based on filter bank method was developed.

On the other hand, a Japanese satellite based augmentation system, MSAS (MTSAT Satellite-based Augmentation System), which is compatible with the United States WAAS and the European EGNOS systems, has been developed by the Japan Civil Aviation Bureau (JCAB), and is planned to be operational in 2007. The MSAS ground infrastructure, consisting of two Master Control Stations (MCS) and four Ground Monitor Stations (GMS) located in Japan and two Monitor Ranging Stations (MRS) in Hawaii and Australia (Fig. 1), is complete and is undergoing operational verification. Two MTSAT satellites, which are space components of MSAS, are already in orbit, and their signals are under examination. The test signal of MSAS can be received and used by commercial GPS/WAAS receivers, however, cannot be used for aircraft operation so far.

Prior to operation, JAXA has conducted flight experiments in order to collect the MSAS test data for research purposes. By using these data, horizontal protection level (HPL) was computed based on GPS/INS filter bank algorithm (Young, et al., 2003), and compared to the HPL_{SBAS} , which was computed based on MOPS for GPS/WAAS airborne equipment (RTCA, 2006).

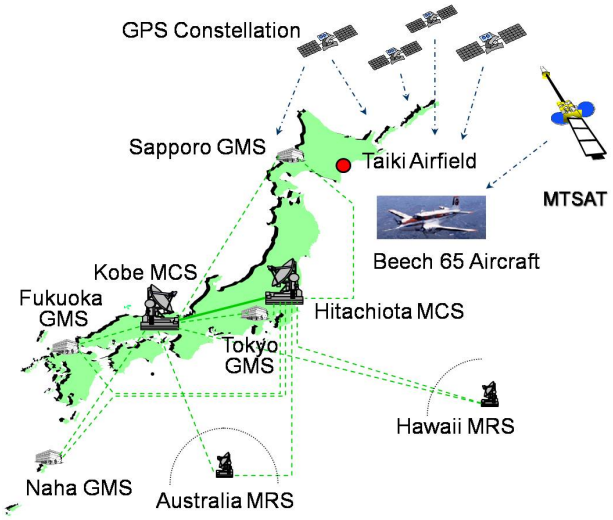

Fig. 1 MSAS and Flight Experiment Overview

2. GPS AIDED INERTAL NAVIGATION AVIONICS

GAIA GPS/INS integrated navigation system was originally developed by the National Aerospace Laboratory (NAL) and the National Space Development Agency of Japan (NASDA) for the High Speed Flight Demonstration (HSFD) project, a test program for the planned HOPE-X space plane (Harigae, et. al, 2001, Nishizawa, et al., 2001). (NAL and NASDA, and another organization, Institute for Space and Astronautical Science (ISAS), were merged into JAXA in October 2003.) A key objective of the HSFD Phase I experiment was to examine automatic takeoff and landing technology using carrier-phase DGPS/INS (CDGPS/INS) integrated navigation, and high accuracy at the level of

Category III approach and landing was demonstrated in differential mode. The onboard avionics has a Kearfott T-24 Inertial Measurement Unit (IMU) with ring laser gyro and servo accelerometer, an Ashtech G12 single-frequency GPS receiver, and a DX4 (66MHz) CPU for navigation processing. Fig. 2 shows a photograph of the GAIA and Table 1 gives its specifications.

Fig. 2 GAIA (Right, Left is an uplink receiver for DGPS)

Table 1. Specifications of GAIA

Item	Spec.
Size	H180mm x W180mm x D280mm
Weight	9.8 kg
Power	46 W (28VDC)
Functions	CDGPS/INS, GPS/INS, INS,
Environment	Temperature: -40 – +55 degree Celsius
	Altitude: 0 – 32 km
	Humidity: <85%
	Acceleration: 8G
	Shock: 15G (11 ms half sine)
	Vibration: 0.04 G^2/Hz (15–1000 Hz), 8.03Grms
Interface	MIL-STD-1553B
Data rate	50 Hz
Reliability	MTBF: more than 3,700 hour

GAIA is currently installed in JAXA's experimental aircraft Beechcraft Model 65 QueenAir and provides navigation data for research purposes. Since GAIA was not capable to decode MSAS message, an Ashtech DG16 GPS/WAAS receiver was installed for this flight test. Onboard equipment system is depicted in Fig. 3.

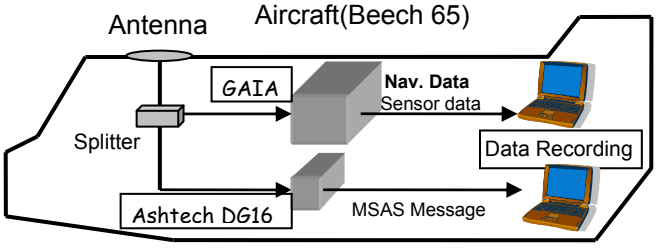

Fig. 3 Onboard Equipment System

The data recorded onboard were used for offline analyses. The processing software was originally developed for MSAS-GAIA (Tomita el al., 2003) and modified to add integrity monitoring function. MSAS-GAIA is a further development of GAIA which utilizes SBAS capability.

3. NAVIGATION ALGORITHMS

The navigation algorithm of GAIA GPS/MSAS/INS is outlined in Fig. 4. GAIA adopts a tightly-coupled GPS/INS integrated navigation algorithm that corrects IMU errors (acceleration and angular rate) as well as the INS navigation results (position, velocity and attitude) using GPS data, and avoids the divergence of inertial navigation (Harigae, et. al, 1998). GAIA has three navigation modes — INS, CDGPS/INS and GPS/INS — and automatically changes between these modes to obtain the most accurate navigation results. For example, if no GPS signal is available, GAIA works in the INS mode. The navigation mode then changes to GPS/INS mode at the acquisition of GPS signals, and to CDGPS/INS mode when RTCM messages (Type 3, 18 and 19) are received. However, only GPS/INS and GPS/MSAS/INS mode were evaluated in this paper since ground differential receiver was not used for the experiment.

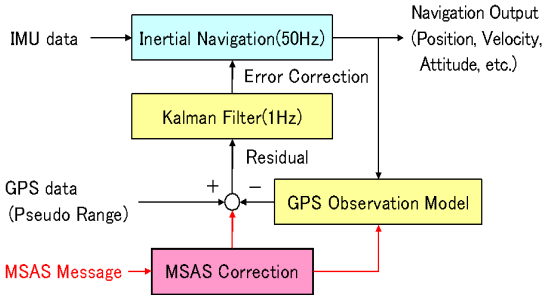

Fig. 4 Outline of GPS/MSAS/INS Navigation Algorithm

GAIA uses a Kalman filter to estimate the inertial navigation error. The error dynamics and measurement equation are subsets of the CDGPS/INS algorithm and are described below.

Error dynamics model

The error dynamics model is as follows:

$$\dot{\boldsymbol{x}} = \boldsymbol{F}\boldsymbol{x} + \boldsymbol{w} \tag{1}$$

$$\mathbf{x} = (\delta\mathbf{r}, \delta\mathbf{v}, \delta\mathbf{e}, \mathbf{b}_{acc}, \mathbf{b}_{gyro}, \mathbf{b}_{clk})^T \tag{2}$$

$$\mathbf{F} = \begin{pmatrix} \mathbf{F}_{rr} & \mathbf{F}_{rv} & \mathbf{0} & \mathbf{0} & \mathbf{0} & \mathbf{0} \\ \mathbf{F}_{vr} & \mathbf{F}_{vv} & \mathbf{F}_{ve} & \mathbf{F}_{vb} & \mathbf{0} & \mathbf{0} \\ \mathbf{F}_{er} & \mathbf{F}_{ev} & \mathbf{F}_{ee} & \mathbf{0} & \mathbf{F}_{eb} & \mathbf{0} \\ \mathbf{0} & \mathbf{0} & \mathbf{0} & \mathbf{F}_{ba} & \mathbf{0} & \mathbf{0} \\ \mathbf{0} & \mathbf{0} & \mathbf{0} & \mathbf{0} & \mathbf{F}_{bg} & \mathbf{0} \\ \mathbf{0} & \mathbf{0} & \mathbf{0} & \mathbf{0} & \mathbf{0} & \mathbf{F}_{bc} \end{pmatrix} \tag{3}$$

$$\mathbf{w} = (\mathbf{0}, \mathbf{0}, \mathbf{0}, \mathbf{w}_{ba}, \mathbf{w}_{bg}, \mathbf{w}_{bc})^T \tag{4},$$

where $\delta\mathbf{r}, \delta\mathbf{v}, \delta\mathbf{e}$ are the position, velocity and attitude error vectors respectively; b_{acc} and b_{gyro} are the accelerometer bias and gyro bias vectors; and b_{clk} is the GPS receiver clock error vector (clock bias and clock drift). The dynamics models of each error component are the same as that of conventional DGPS/INS hybrid navigation. The reference frame of the system matrix F is the navigation frame.

Measurement equation model

For INS calibration, GAIA uses the pseudo-range and SBAS correction data broadcast in the MSAS messages. The following measurement model is used for the pseudo-range:

$$\rho_c = |\mathbf{r} - \mathbf{r}_{sv} + \delta\mathbf{r}_{sv}| + b_{clk\_sv} + \delta b_{clk\_sv} + b_{sag} + b_{ion} + b_{trop} + b_{clk} \quad (5),$$

where ρ_c is the computed pseudo-range; r, r_{sv} are the position vectors of the user and the GPS satellite respectively; $\delta\mathbf{r}_{sv}$ is the satellite position error in the MSAS long-term satellite error corrections; b_{clk_sv} is the satellite clock error calculated using the GPS navigation message; δb_{clk_sv} is the clock error in the MSAS long-term satellite error corrections; b_{sag} is the Sagnac effect; b_{ion} and b_{trop} are the ionospheric and tropospheric delays. The calculation of MSAS error correction and ionospheric and tropospheric delays is specified in the RTCA MOPS (RTCA-DO229D).

The measurement error is then calculated as follows, and input to the Kalman filter:

$$\Delta\rho = \rho_{measured} + \mathrm{PRC} - \rho_c \quad (6),$$

where PRC is the fast pseudo-range correction in the MSAS message.

4. FDE ALGORITHMS

Among several FDE algorithms proposed for GPS/INS navigation system, normalized solution separation method using filter bank was adopted to our prototype software. The algorithm is summarized below.

The discrete state model and measurement model of the full filter are described as:

$$\mathbf{x}_0(k) = \Phi_0(k, k-1)\mathbf{x}_0(k-1) + \boldsymbol{\omega}_0(k) \quad (7)$$

$$\mathbf{z}(k) = H_0(k)\mathbf{x}_0(k) + \mathbf{v}_0(k) + \mathbf{b}(k)u(k, k_0) \quad (8),$$

where $x_0(k)$ is a GPS/INS error state, z(k) is a GPS observation vector. $\boldsymbol{\omega}_0(k)$ and $v_0(k)$ are Gaussian white noises whose covariances are $Q_0(k)$ and $R_0(k)$. H_0 and Φ_0 are measurement matrix and transition matrix. $\boldsymbol{b}(k)$ models j-th satellite failure (i.e., $\boldsymbol{b}(k)=b(k)\mathbf{e}_j$). $u(k,k_0)$ is the unit step function at k_0 (i.e., u=1 for $k \geqq k_0$) where k_0 is the time at which the failure occurs.

When the j-th measurement is excluded, the measurement equation for subfilter is described as follows

$$\mathbf{z}_j(k) = E_j\mathbf{z}(k), \quad E_j = I_n - \mathbf{e}_j\mathbf{e}_j^T \quad (9).$$

The initial condition and covariance for both full filter and j-th subfilter are

$$\hat{\mathbf{x}}_0(0) = \hat{\mathbf{x}}_j(0) = E[\mathbf{x}(0)] \quad (10)$$

$$P_0(0) = P_j(0) \quad (11).$$

Now, horizontal solution separation vector is defined as:

$$\boldsymbol{\beta}_j(k) = \hat{\mathbf{x}}_0^h(k/k) - \hat{\mathbf{x}}_j^h(k/k) = \tilde{\mathbf{x}}_0^h(k) - \tilde{\mathbf{x}}_j^h(k) \quad (12),$$

where $\hat{\mathbf{x}}_0^h$ and $\hat{\mathbf{x}}_j^h$ are horizontal position error estimate for fullfilter and j-th subfilter, while $\tilde{\mathbf{x}}_0^h$ and $\tilde{\mathbf{x}}_j^h$ are the estimation error for fullfilter and j-th subfilter, respectively. The covariance of solution separation vector is described as

$$B_j(k) = P_j^h(k/k) - P_0^h(k/k) \quad (13),$$

and normalized solution separation test static is given by

$$\lambda_j(k) = \boldsymbol{\beta}_j^T(k)B_j^{\#}(k)\boldsymbol{\beta}_j(k) \quad (14),$$

where $B_j^{\#}$ is the Moore-Penrose generalized inverse of the B_j matrix. λ_j is chi-square distributed and used for fault detection. When a failure occurs, λ_j is non-central chi-square distributed and non-centrality parameter is denoted as 'Pbias' in parity-space FDE algorithms (Brown et al., 1997). The presence of any bias vector with a magnitude greater than Pbias, will be detected with $(1-P_{MD})$ probability, where P_{MD} is probability of missed detection.

The HPL is determined as follows:

$$HPL = \max\{HPL_{H0}, HPL_{H1}\} \quad (15),$$

where HPL_{H0} is based on the rare normal fault-free hypothesis, and HPL_{H1} is based on the fault-in-progress hypothesis. HPL_{H0} and HPL_{H1} are given by as follows:

$$HPL_{H0} = K_{ffd}\sqrt{\sigma_{1,0}} \quad (16)$$

$$HPL_{H1} = \max_{i=1}^{N}\left\{pbias\sqrt{\sigma_{1,Bj}} + K_{cep,j}\sqrt{\sigma_{1,j}} + K_{cep,Bj}\sqrt{\sigma_{1,Bj}}\right\} \quad (17),$$

where $\sigma_{1,0}$ and $\sigma_{2,0}$ are the eigenvalues of P_0^h, $\sigma_{1,0} \geq \sigma_{2,0}$, K_{ffd} is a function of (1-P_{H0}) probability and $\sqrt{\sigma_{1,0}/\sigma_{2,0}}$ in the CEP look-up table, and P_{H0} is the fault-free integrity probability. Similarly, $\sigma_{1,j}$, $\sigma_{1,Bj}$ are larger eigenvalues of P_j^h and B_j, respectively, and $K_{cep,j}$, $K_{cep,Bj}$ are functions of (1-P_{MD}) probability and $\sqrt{\sigma_{1,j}/\sigma_{2,j}}$, $\sqrt{\sigma_{1,Bj}/\sigma_{2,Bj}}$ in the CEP look-up table.

In the analyses later, HPL are computed for en route through LNAV approach. Therefore, probability of missed alert, which is assumed to be equivalent with P_{MD}, false alert rate, and fault-free integrity probability are 0.001, 10^{-5}/hour, and 10^{-5}/hour, respectively. The HPL computed as above is denoted as HPL_{FD} hereafter.

5. FLIGHT EXPERIMENT AND RESULTS

The flight experiment was carried out on July 23, 2007 at Taiki airfield in Hokkaido, northern Japan (see Fig. 1). The Beech 65 aircraft took off from Obihiro Airport, about 40 km north west of Taiki, flew to Taiki airfield and carried out lots of circling patterns with up to 30 degree bank above the airfield and Pacific Ocean coastline, then went back to Obihiro airport. The trajectory of Beech 65 is shown in Fig. 5 and height profile is shown in Fig.6.

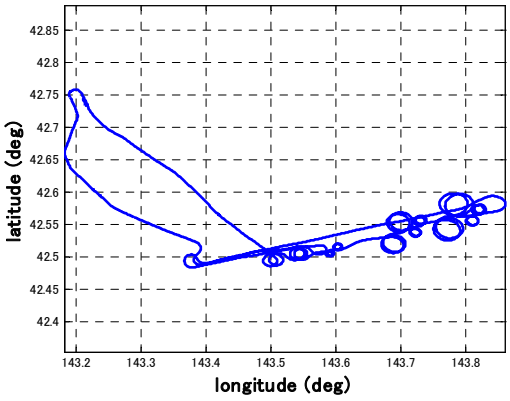

Fig. 5 Trajectory of Aircraft

Ellipsoidal height of Obihiro airport was about 180 meters. Flight duration was about one hour and 35 minutes. The origin of time was power/on of GAIA and the profile after the alignment of INS, which took about 10 minutes, was depicted. The change of roll angle is shown in Fig. 7 since it gives information of satellite blocking.

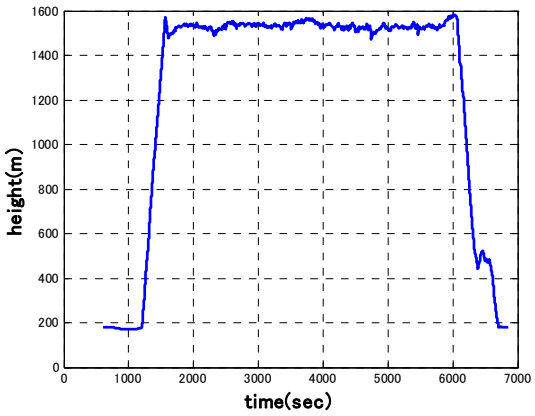

Fig. 6 Height Profile

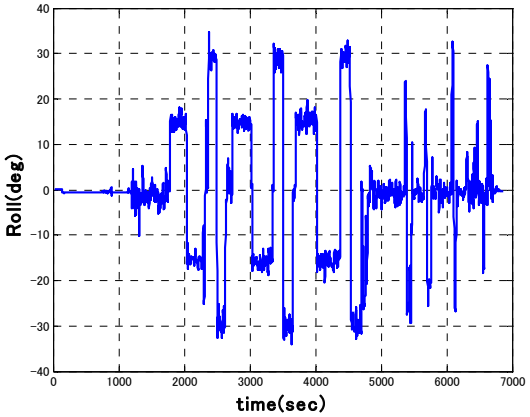

Fig. 7 Roll Angle

Estimated horizontal and vertical position error (95%) of navigation full filter, which are computed from P_0, with/without MSAS corrections are shown in Fig. 8 and Fig. 9.

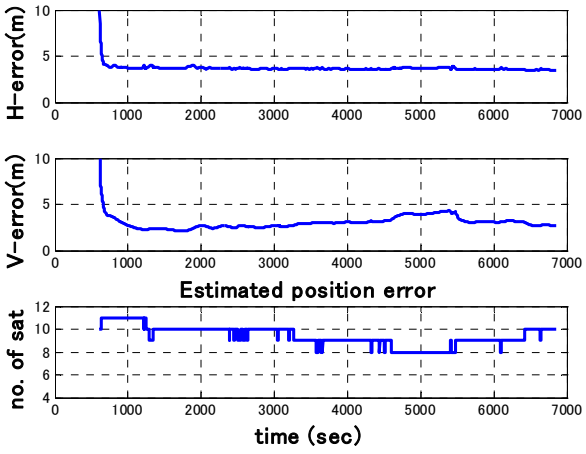

Fig. 8 Estimated Position Error (95%) in GPS/INS and Number of satellites

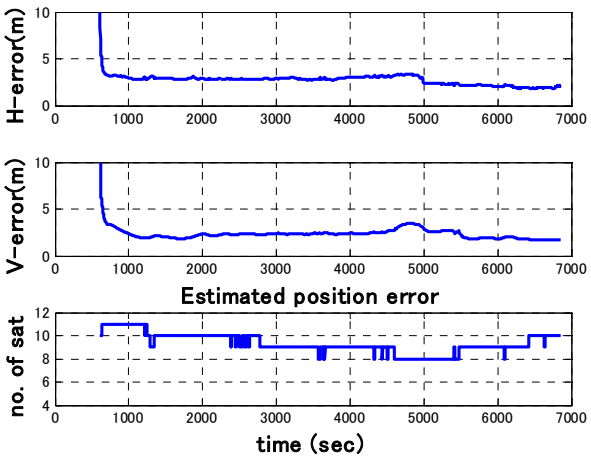

Fig. 9 Estimated Position Error (95%) in GPS/MSAS/INS and Number of satellites

Since there was no ground differential receiver, reference trajectory (e.g. KGPS trajectory) was not obtained. However, compared with former evaluation of positioning accuracy of MSAS-GAIA, these results seem reasonable.

Before evaluating horizontal protection level, measurement error of GPS pseudorange was checked. Since range error variances were used as weights both in GPS/INS navigation filter and in HPL_{FD}/HPL_{SBAS} calculation, they were key factors which determined magnitude of HPL. The range error variance for i-th satellite is represented as:

$$\sigma_i^2 = \sigma_{i,flt}^2 + \sigma_{i,UIRE}^2 + \sigma_{i,air}^2 + \sigma_{i,trop}^2 \qquad (18),$$

where $\sigma_{i,flt}^2$, $\sigma_{i,UIRE}^2$, $\sigma_{i,air}^2$, $\sigma_{i,trop}^2$ are variance of fast/long term correction residuals, ionospheric delay, airborne receiver error, and tropospheric error, respectively. The methods to calculate these terms are described in Appendix J of DO-229D for both cases with/without SBAS message, and among these, the ionospheric delay error variance is the major factor. The calculated range error (σ_i) for each GPS satellite are shown in Fig.10 and Fig. 11.

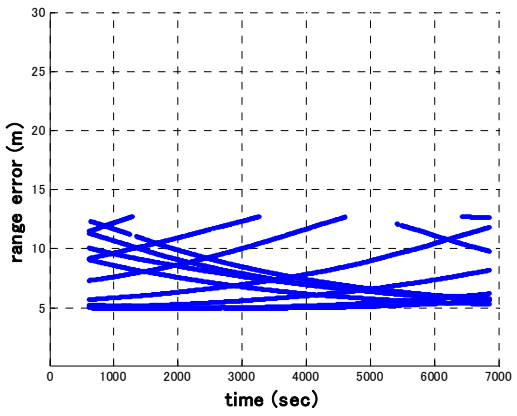

Fig. 10 Calculated Range Error of GPS

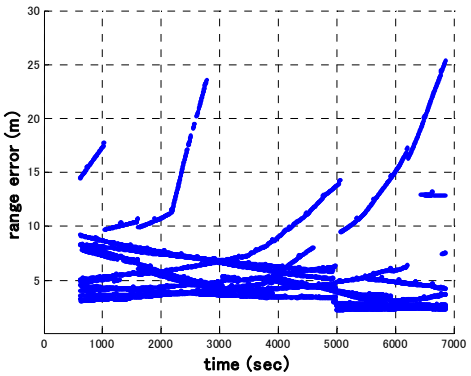

Fig. 11 Calculated Range Error of GPS Corrected by MSAS message

The calculated range errors of GPS without MSAS correction (Fig. 10) were larger than five meters in most of the time. On the other hand, when pseudoranges were corrected by MSAS message (Fig. 11), many satellites had range errors less than five meters, especially after a lapse of 5000 seconds. A few satellites showed range errors larger than uncorrected cases in some parts. Since the test field was located close to north eastern border of Japan, accuracy of estimated ionospheric delay at grid point (GIVE) was degraded. Nevertheless, these data may not degrade the performance of navigation filter and HPL since there were sufficient satellites and bad data were just lightly weighted. Calculated HPL_{FD} and HPL_{SBAS} without MSAS correction are shown in Fig. 12.

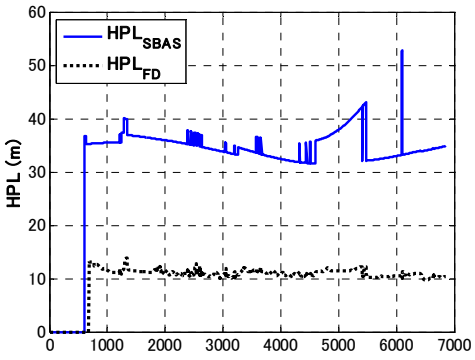

Fig. 12 HPL without MSAS Correction

It is clear that integrating GPS with INS drastically reduces the value of HPL. Also, HPL_{FD} seemed very stable while HPL_{SBAS} was affected by the number of satellites and resulting satellite geometry. This superior performance is basically attributed to accurate position estimate of navigation filter. HPL_{SBAS} was directly affected by the range error variance calculated by Eq.18, which was very conservative for safety reason. On the other hand, HPL_{FD} was calculated based on the filter covariance, which was smooth and small due to the effects of hybridization with INS. Therefore, HPL_{FD} was reduced even though the same value of range error variance was used.

The HPL_{FD} and HPL_{SBAS} when pseudoranges were corrected by using MSAS message were shown in Fig. 13. Compared

to Fig. 12, HPL_{SBAS} was improved since GPS range errors were reduced. On the other hand, improvement of HPL_{FD} by MSAS correction was not significant except after a lapse of about 5400 seconds.

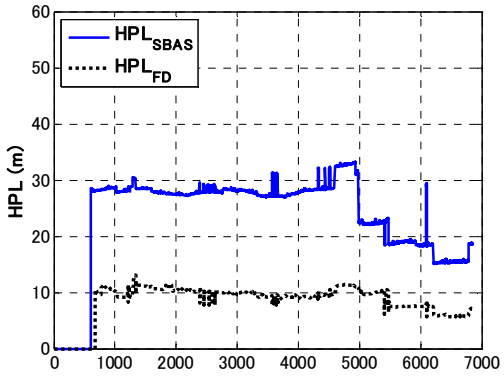

Fig. 13 HPL with MSAS Correction

In order to see the effect of satellite outage, satellite mask angle was changed as 20 degrees, though it was set as 10 degrees in the previous processing. Calculated HPL_{FD} and HPL_{SBAS} are shown in Fig. 14 (without MSAS correction) and Fig. 15 (with correction).

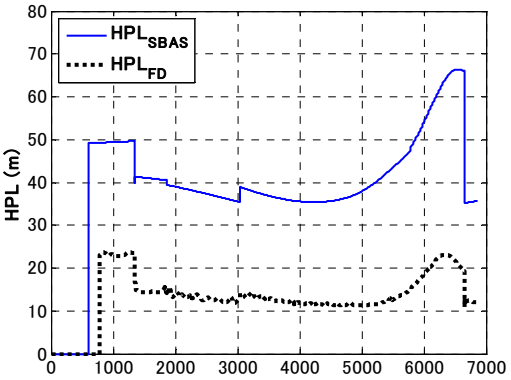

Fig. 14 HPL without MSAS Correction (Mask: 20 deg)

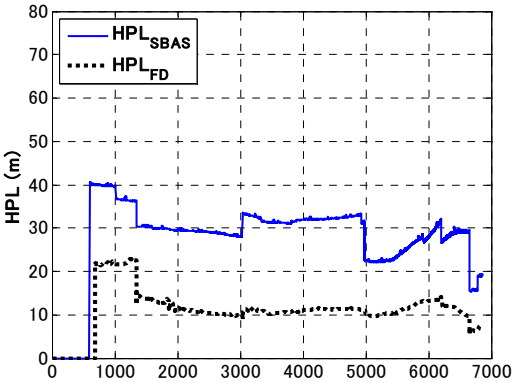

Fig. 15 HPL with MSAS Correction (Mask: 20 deg)

Note that vertical scales are different from Fig 12 and 13. It was demonstrated that GPS/INS based HPL was robust even if number of satellites was reduced. Also, MSAS correction was effective in reducing HPL.

6. CONCLUDING REMARKS

A FDE function using filter bank was implemented into the navigation software of JAXA's GPS/INS avionics, GAIA. A flight experiment was conducted and offline analyses using collected data of GPS , MSAS, and INS were carried out. As results, HPL_{FD} based on GPS/INS was much better than HPL_{SBAS}, which was calculated by using GPS only or GPS with MSAS correction.

In this paper, the HPL for only en route through LNAV approach was investigated. The next step is to investigate the effect of GPS/MSAS and INS hybridization for precision approach. Since there is no technical standard for GPS/INS for the use of precision approach, the reduction of HPL/VPL would not directly lead to commercialization of GPS/INS for precision approach. Further research, development and evaluation will be conducted to assess the potential of GPS/INS for practical use.

REFERENCES

Brown, R. G. and Chin, G. Y. (1997). GPS RAIM: Calculation of Threshold and Protection Radius Using Chi-Square Methods - A Geometric Approach. In: *NAVIGATION (Red Book Series)*, **5**, pp.155-178.

Harigae, M., Tsujii, T., Ono, T., Inagaki, T. and Tomita, H. (1998). Flight Evaluation of Carrier DGPS/INS Hybrid Navigation for Automatic Landing. *Proceedings of the 11th International Technical Meeting of the Satellite Division of the Institute of Navigation*, pp. 437–446.

Harigae, M., Nishizawa, T. and Tomita, H. (2001). Development of GPS Aided Inertial Navigation Avionics for High Speed Flight Demonstrator. *Proceedings of the 14th International Technical Meeting of the Satellite Division of the Institute of Navigation*, pp. 2665–2675.

Nishizawa, T., Sagisaka, M., Inokuchi, H. and Harigae, M. (2001). Avionics Architecture for HOPE-X High Speed Flight Demonstrator. *Proceedings of AIAA/NAL-NASDA-ISAS 10th International Space Planes and Hypersonic Systems and Technologies Conference*, 24-27 April 2001, AIAA-2001-1835.

RTCA Working Group SC-159 (2006). Minimum Operational Performance Standards for Global Positioning System / Wide Area Augmentation System Airborne Equipment. Document No. RTCA/DO-229D.

Tomita, H., Harigae, M. and Hoshinoo, K. (2003). Flight Evaluation of GPS Aided Inertial Navigation Avionics with MSAS Augmentation (MSAS-GAIA). *Proceedings of the 16th International Technical Meeting of the Satellite Division of the Institute of Navigation*, pp. 2819–2827.

Young, R. S. and G. A. McGraw (2003). Fault Detection and Exclusion Using Normalized Solution Separation and Residual Monitoring Methods. *Navigation*, **50**, No.3, pp. 151-169.